

Molecular Dynamics Computer Simulation of Crystal Growth and Melting in $\text{Al}_{50}\text{Ni}_{50}$

A. KERRACHE¹, J. HORBACH^{1,2} and K. BINDER¹

¹ *Institut für Physik, Johannes Gutenberg–Universität Mainz, Staudinger Weg 7, 55099 Mainz, Germany*

² *Institut für Materialphysik im Weltraum, Deutsches Zentrum für Luft– und Raumfahrt (DLR), 51170 Köln, Germany*

PACS 81.10.Aj – Theory and models of crystal growth; physics of crystal growth, crystal morphology and orientation
 PACS 64.70.Dv – Solid-liquid transitions
 PACS 02.70.Ns – Molecular dynamics and particle methods

Abstract. – The melting and crystallization of $\text{Al}_{50}\text{Ni}_{50}$ are studied by means of molecular dynamics computer simulations, using a potential of the embedded atom type to model the interactions between the particles. Systems in a slab geometry are simulated where the B2 phase of AlNi in the middle of an elongated simulation box is separated by two planar interfaces from the liquid phase, thereby considering the (100) crystal orientation. By determining the temperature dependence of the interface velocity, an accurate estimate of the melting temperature is provided. The value $k = 0.0025 \text{ m/s/K}$ for the kinetic growth coefficient is found. This value is about two orders of magnitude smaller than that found in recent simulation studies of one-component metals. The classical Wilson-Frenkel model is not able to describe the crystal growth kinetics on a quantitative level. We argue that this is due to the neglect of diffusion processes in the liquid-crystal interface.

Introduction. – The classical model for crystallization from the melt is the one proposed by Wilson [1] and Frenkel [2]. It considers crystal growth as an activated process, controlled by the mass transport in the liquid. However, various studies using molecular dynamics (MD) computer simulation have shown that the Wilson-Frenkel scenario is not applicable to a large class of materials. Especially in pure metals, growth kinetics is much faster than expected for an activated diffusion-limited mechanism [3–14]. In this case, rearrangements in the liquid structure are not required to provide the formation of crystalline layers. This may explain why one-component metals are not glassforming systems in general. On the other hand, binary metallic alloys are known as glassforming systems, provided that heterogeneous nucleation can be avoided. Indeed, these systems exhibit in general a much slower growth kinetics than pure metals. Recent studies have demonstrated that the MD simulation technique is well-suited to elucidate the crystallization kinetics in binary alloys [15–21]. But these studies show also that the growth kinetics in binary mixtures is more complicated than in the one-component counterparts. One of

the open questions is to what extent the Wilson-Frenkel picture is valid for two-component metals. This question is addressed in the following.

In this work, the crystal growth kinetics of the binary alloy $\text{Al}_{50}\text{Ni}_{50}$ is investigated by MD simulation. The experimental melting temperature for this system is at 1920 K where it exhibits a first order phase transition from a liquid to an intermetallic B2 phase. Very recently, the crystal growth velocity for this transition has been measured by Reutzler *et al.* [22] using an electromagnetic levitation technique under reduced gravity conditions in combination with a high-speed camera. At an undercooling of about 60 K, growth velocities of the order of 0.1 m/s were found. This value is about two orders of magnitude smaller than that found for pure metals at comparable undercoolings, indicating that $\text{Al}_{50}\text{Ni}_{50}$ may be the prototype of a system with a diffusion-limited growth mechanism.

The MD simulation allows for an accurate determination of the melting temperature, kinetic growth coefficients, and transport coefficients such as self- and interdiffusion constants. These information are required to check the validity of the Wilson-Frenkel model of crystal growth.

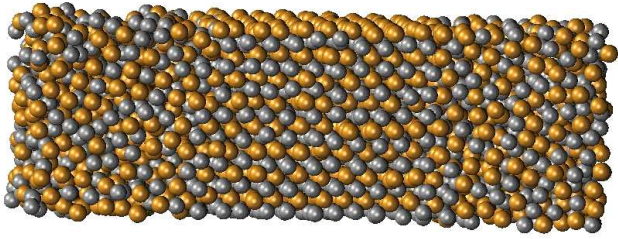


Fig. 1: Snapshot of a simulated configuration with two crystal-melt interfaces of the system $\text{Al}_{50}\text{Ni}_{50}$ at the temperature $T = 1500$ K. Al and Ni atoms are shown as grey and brown spheres, respectively.

As we shall see below the kinetic growth coefficient, as estimated by our simulation for the (100) orientation of the crystal, is indeed much smaller than that found for simple metals. Thereby, the growth velocities are in good agreement with those measured in the aforementioned experiment by Reutzler *et al.* [22]. However, we demonstrate that the Wilson-Frenkel model is not able to describe the crystal growth kinetics in $\text{Al}_{50}\text{Ni}_{50}$ on a quantitative level, at least for plausible choices of the various free parameters appearing in the theory. This indicates the need of microscopic theories on the various aspects of crystal growth kinetics. By computing diffusion profiles for an inhomogeneous crystal-liquid system at coexistence, we show explicitly that such theories have to take into account diffusion processes in the crystal-liquid interface region.

Details of the simulation. – To investigate the crystallization of $\text{Al}_{50}\text{Ni}_{50}$ from the melt, we have done extensive molecular dynamics computer simulations. The interactions between the atoms were modelled by a potential of the embedded atom type, proposed by Mishin *et al.* [23]. Recent studies have shown that this potential gives a realistic description of the diffusion dynamics in Al-Ni melts [24, 25]. The simulations were done at constant pressure ($p_{\text{ext}} = 0$). For this, an algorithm proposed by Andersen was used, setting the mass of the piston to 0.0027 u [26]. Temperature was kept constant by coupling the system at every 100 steps to a stochastic heat bath. The equations of motion were integrated with the velocity form of the Verlet algorithm [27] with a time step of 1 fs.

At each temperature in the range $1600 \text{ K} \geq T \geq 1200 \text{ K}$, 12 independent samples with solid-liquid interfaces were prepared. To this end, the B2 phase of $\text{Al}_{50}\text{Ni}_{50}$ was equilibrated at the target temperature for 1 ns. The simulations were done for a system of $N = 3072$ particles ($N_{\text{Al}} = N_{\text{Ni}} = 1536$) in an elongated simulation box of size $L \times L \times L_z$ (with $L_z = 3 \times L$), considering the (100) direction of the crystal. Periodic boundary conditions were employed in all three spatial directions. Having relaxed the crystal sample, one third of the particles in the middle of the box were fixed and the rest of the system was melted during 500 ps at $T = 3000$ K. Then, the whole system was annealed at the target temperature for another

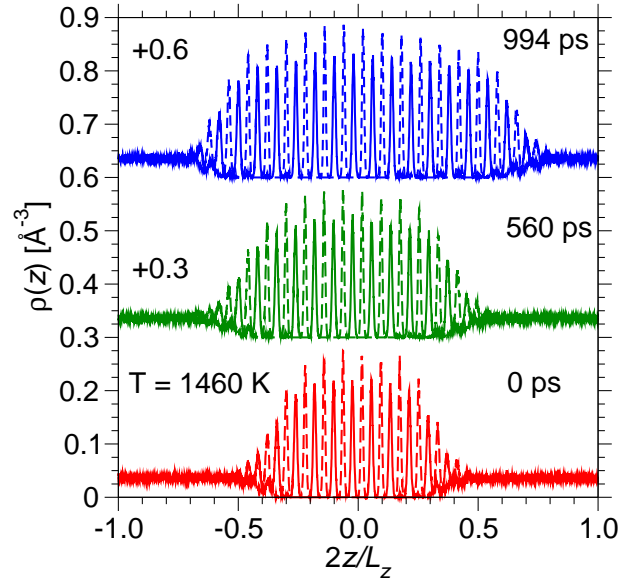


Fig. 2: Number density profiles during crystal growth at $T = 1460$ K for Al (solid lines) and Ni (dashed lines). The profiles corresponding to $t = 560$ ps and $t = 994$ ps are shifted with respect to the $t = 0$ ps profiles by 0.3 \AA and 0.6 \AA , as indicated.

500 ps, before we started the production runs over 1 ns in the NpT ensemble. A snapshot of the system with two interfaces at $T = 1500$ K is shown in Fig. 1. We did also 20 independent microcanonical runs of the crystal-liquid system at the coexistence temperature $T = 1520$ K (see below), starting from fully equilibrated samples. These runs, each of them over 1 ns, was used to study the diffusion dynamics in the crystal-liquid interface region.

In addition, simulations of liquid samples were performed at the temperatures $T = 1200$ K, 1300 K, 1400 K, 1500 K, 1600 K, 1800 K, and 2000 K, in order to determine self-diffusion coefficients as well as the interdiffusion coefficient (see below). In this case, systems of 2000 particles were placed in a cubic simulation box. At each temperature, equilibration runs over 1 ns were done in the NpT ensemble, followed by microcanonical production runs over 23 ns.

Results. – As described in the previous section, samples in an elongated simulation box were prepared as starting configurations where the crystal in the middle is surrounded by the liquid phase on both sides, separated by two interfaces (see Fig. 1). The behavior of these samples depends strongly on the temperature at which they are simulated. While below the melting temperature T_m , the crystal will grow (as shown in Fig. 2), it will melt above T_m . From the simulation, the velocity v_I with which the liquid-crystal interface moves can be determined. At $T = T_m$, the interface velocity v_I vanishes. Thus, by the extrapolation $v_I \rightarrow 0$ the melting temperature T_m can be estimated. In the following, we show that this procedure yields a rather accurate estimate of T_m . Then, we demonstrate that the crystal growth mechanism in $\text{Al}_{50}\text{Ni}_{50}$ can

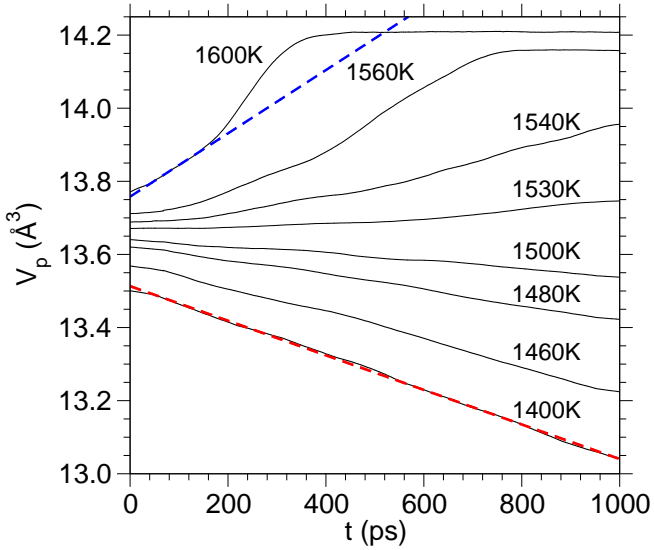


Fig. 3: Volume per particle, V_p as a function of time for different temperatures, as indicated. The bold dashed lines are examples of linear fits from which the volume velocity \dot{V} is determined.

be elucidated by investigating the diffusion dynamics in the liquid phase and in the crystal-liquid interface region.

Figure 2 displays the partial number density profiles $\rho(z)$ of Al and Ni at $T = 1460$ K along the z direction, i.e. perpendicular to the solid-liquid interfaces. The lower profiles in Fig. 2 correspond to the starting configuration, while the second and the third ones correspond to $t = 560$ ps and 994 ps. Note that in Fig. 2 the z coordinate is scaled by the factor $2/L_z$, placing $z = 0$ in the middle of the simulation box. Whereas the crystal structure leads to pronounced peaks in $\rho(z)$, a constant density is observed for the liquid regions along the z direction, as expected. We can also infer from Fig. 2 that the intermetallic B2 phase [here in (100) orientation] exhibits a pronounced chemical ordering, characterized by the alternate sequence of Al and Ni layers. This indicates that, different from one-component metals, the crystal growth kinetics relies on local rearrangements in the liquid structure. Thus, one may expect that diffusive transport is required to bring the atoms of each species to a suitable site in the B2 crystal. As one can further see in Fig. 2, the crystal is growing at $T = 1460$ K. Thus, this temperature is below the melting temperature of our $\text{Al}_{50}\text{Ni}_{50}$ model.

Since the density of the crystalline B2 phase is higher than that of the liquid phase, the total volume of the system decreases at temperatures $T < T_m$ whereas it increases above T_m . Figure 3 shows the time dependence of the volume per particle, V_p , for different temperatures between 1400 K and 1600 K. From this plot, one can infer that the melting temperature is between 1500 K and 1530 K. Also shown in Fig. 3 are examples of linear fits of the form $f(t) = A - \dot{V}_p t$. Such linear growth laws are expected for steady state growth [7]. We use these fits

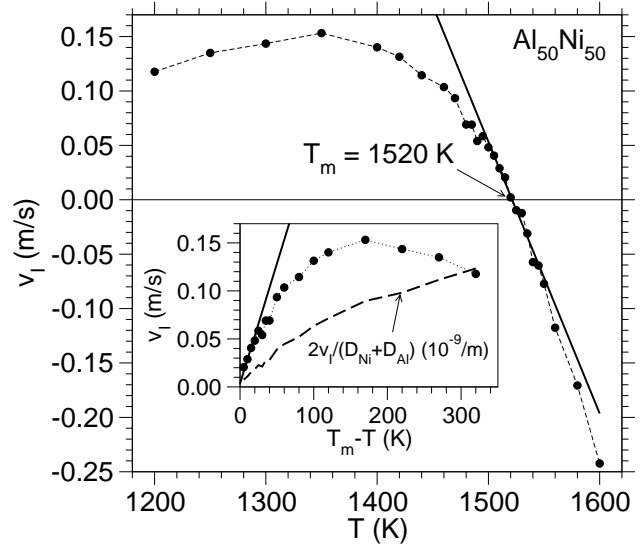


Fig. 4: Interface velocity as a function of temperature (filled circles, the dashed line is a guide to the eye). The bold line is a linear fit, $v_I = k(T_m - T)$, yielding the kinetic growth coefficient $k = 0.0025$ m/s/K and the melting temperature $T_m = 1520$ K. The inset shows the interface velocity as a function of undercooling $T_m - T$ and the interface velocity divided by the averaged self-diffusion coefficient (dashed line).

to determine the change of the volume \dot{V} per unit time. The deviations from the linear behavior at short times reveal that the growth (or melting) of the crystal is not yet in a steady state regime [7]. At high temperatures, we see a complete melting of the crystal and thus the volume V_p reaches a constant at long times corresponding to the specific volume of the liquid phase. Prior to this, the melting of the crystal is faster than in the linear steady-state regime. In this intermediate regime the crystal has shrunk to such small dimensions that we see essentially the interaction between the two interfaces in the simulation box and thus strong deviations from steady state growth are observed.

From the volume change \dot{V}_p , the velocity v_I , with which the liquid-crystal interfaces move, can be estimated as follows:

$$v_I = \frac{\dot{V}_p}{2N_1(V_c - V_l)} d \quad (1)$$

Here, the product $N_1(V_c - V_l)$ quantifies the increase of the volume caused by the addition of a crystalline layer (with N_1 the average number of particles in a layer, and V_c and V_l the specific volumes of the crystal and the liquid phase, respectively). The length d is the spacing between crystalline layers.

Figure 4 displays the interface velocity v_I as a function of temperature. We see that v_I vanishes around 1520 K and thus this temperature is the estimate for the melting temperature, T_m , of our simulation model. Note that the experimental value for T_m is around 1920 K and so our simulation underestimates the experimental value by

about 20%. Around T_m , the simulation data for v_I can be fitted by the linear law $v_I = k(T_m - T)$ where the fit parameter k is the so-called kinetic coefficient. The fit, that is shown in Fig. 4, yields the value $k = 0.0025$ m/s/K. This value is about two orders of magnitude smaller than the typical values for kinetic coefficients that have been found in simulations of one-component metals [9–11, 28].

The inset in Fig. 4 shows the interface velocity as a function of undercooling $\Delta T = T_m - T$. We see that v_I increases linearly up to an undercooling of about 30 K. At $\Delta T \approx 180$ K, the interface velocity reaches a maximum value of about 0.15 m/s. Note that at small undercoolings our simulation data are in good agreement with recent experimental data on $\text{Al}_{50}\text{Ni}_{50}$, measured under reduced gravity conditions during a parabolic flight campaign [22]. Also shown in the inset of Fig. 4 is the quantity $2v_I/(D_{\text{Ni}} + D_{\text{Al}})$, with D_{Ni} and D_{Al} the self-diffusion constants of Ni and Al, respectively. The self-diffusion constants will be discussed in detail below. Here, we note that the maximum in v_I disappears when one divides this quantity by the averaged self-diffusion coefficient. Thus, the occurrence of a maximum in $v_I(\Delta T)$ is due to the slowing down of diffusion processes with decreasing temperature.

On a qualitative level, the behavior of $v_I(\Delta T)$ can be understood in the framework of the Wilson-Frenkel model. The model relates the interface velocity to the difference between the rate at which the atoms join the crystal and the rate at which they leave the crystal. As a result the following formula for v_I is obtained [28]:

$$v_I = A_{\text{kin}} \left[1 - \exp\left(-\frac{\Delta g}{k_B T}\right) \right] \quad (2)$$

with A_{kin} a kinetic prefactor, k_B the Boltzmann constant and Δg the free energy difference between the liquid and crystal phase. Close to coexistence, the free energy difference Δg is proportional to ΔT , and the exponential function in Eq. (2) can be approximated, such that $1 - \exp(-\frac{\Delta g}{k_B T}) \approx \frac{l\Delta T}{k_B T T_m}$ with l the latent heat of the liquid-to-solid transition. Furthermore, the kinetic prefactor A_{kin} can be expressed in terms of the diffusion coefficient D of the liquid. Eventually, at small ΔT the expression for v_I can be written as [28]

$$v_I = k_{\text{WF}} \Delta T \quad \text{with} \quad k_{\text{WF}} = \frac{6df}{\Lambda^2} D \frac{l}{k_B T T_m} \quad (3)$$

where f represents the fraction of collisions with the crystal that contribute to the growth of the crystal. The parameter Λ corresponds to an elementary diffusive jump distance of particles in the liquid [28]. Note that it is assumed in the derivation of Eq. (3) that the diffusion constant can be expressed by an Arrhenius law,

$$D = D_0 \exp\left(-\frac{Q}{k_B T}\right) \quad \text{with} \quad D_0 = \frac{1}{6} \Lambda^2 \nu \quad (4)$$

with Q an activation energy associated with the diffusion

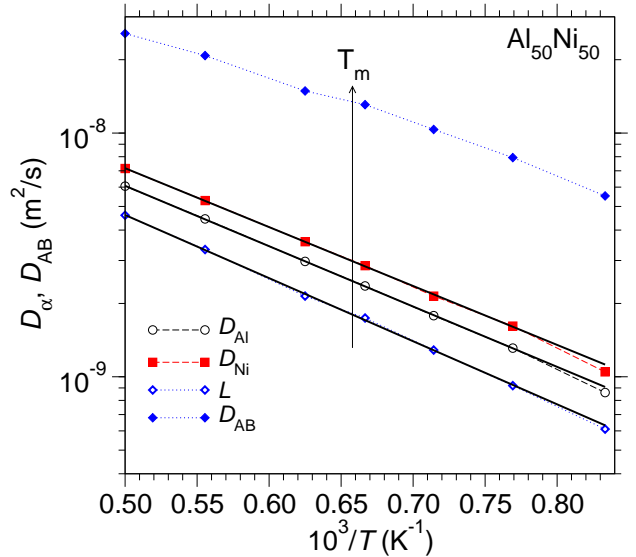


Fig. 5: Arrhenius plot of self-diffusion constants D_α ($\alpha = \text{Al, Ni}$), Onsager coefficient L and interdiffusion constant D_{AB} for $\text{Al}_{50}\text{Ni}_{50}$. The solid lines are fits with the Arrhenius law (4), see text. The arrow indicates the location of the melting temperature $T_m \approx 1520$ K of the simulation model.

of the atoms in the liquid and ν a frequency of the order of the Debye frequency.

In order to check whether the Wilson-Frenkel formula for the kinetic coefficient k_{WF} in Eq. (3) yields quantitative agreement with the value $k = 0.0025$ m/s/K for $\text{Al}_{50}\text{Ni}_{50}$ (see above), we have computed the temperature dependence of self- and interdiffusion coefficients around $T_m = 1520$ K. Whereas the self-diffusion constant D_α is the transport coefficient for tagged particle diffusion of atoms of type α (here $\alpha = \text{Al, Ni}$), the interdiffusion coefficient D_{AB} describes diffusive transport due to concentration fluctuations among the different components. The self-diffusion constants D_α have been computed from the long-time limit of the corresponding mean-squared displacements. The interdiffusion coefficient is given by $D_{\text{AB}} = \Phi L$ where Φ is the so-called thermodynamic factor and L is the Onsager coefficient. The thermodynamic factor expresses the thermodynamic forces to homogenize the mixture with respect to concentration fluctuations. We have calculated this quantity from the $q \rightarrow 0$ limit of the inverse concentration-concentration structure factor (see Ref. [25]). The Onsager coefficient L contains all the kinetic contributions to D_{AB} and can be determined from a generalized mean-squared displacement describing the centre-of-mass motion of one species. For details of the calculation of L and Φ , we refer the reader to a recent publication [25].

An Arrhenius plot of the different diffusion coefficients is shown in Fig. 5. As in a recent simulation study of $\text{Al}_{80}\text{Ni}_{20}$ [25], the interdiffusion coefficient is about a factor 4 to 6 higher than the self-diffusion constants. This is due to the thermodynamic factor (note that the Onsager coef-

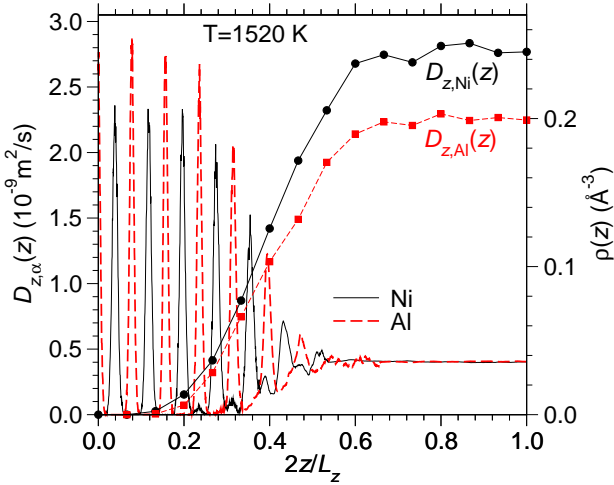


Fig. 6: Number density profiles and diffusion profiles for Ni and Al at coexistence, as indicated.

ficient lies below the self-diffusion constants). The origin of this behavior is a large resistance to macroscopic concentration fluctuations in dense liquids (a similar property of dense liquids is their very low compressibility). With respect to crystal growth kinetics in a binary alloy such as Al₅₀Ni₅₀, it is not clear whether one has to consider self- or interdiffusive transport as the limiting growth mechanism.

Also shown in Fig. 5 are fits with Arrhenius laws (4). From these fits, we obtain the activation energies $Q = 0.49$ eV for D_{Al} , $Q = 0.48$ eV for D_{Ni} , and $Q = 0.51$ eV for L . The prefactors D_0 are 1.05×10^{-7} m²/s, 1.15×10^{-7} m²/s, and 0.91×10^{-7} m²/s for D_{Al} , D_{Ni} , and L , respectively. These values for the prefactors can be compared to those proposed by Eq. (4). With the reasonable choices $\lambda = 3$ Å and $\nu = 6$ THz, similar values for D_0 as in the fits are obtained, i.e. $D_0 \approx 10^{-7}$.

Moreover, the expression (3) for the kinetic coefficient k_{WF} does not predict the order of magnitude correctly. To see this, we can compute the value of k_{WF} at $T_m \approx 1520$ K using the results from the simulation. With $l = 0.23$ eV, $D_\alpha \approx 2 \times 10^{-9}$ m²/s, $\Lambda^2/6 \approx 1.5$ Å², $d = 3$ Å and $f = 1$, the value $k_{\text{WF}} \approx 0.05$ m/s/K is yielded which is about one order of magnitude higher than the value for k , as obtained in our simulation. The result for k_{WF} is even worse if we replace the self-diffusion constant by the interdiffusion constant in our estimate. In this case, we find $k_{\text{WF}} \approx 0.25$ m/s/K.

But why does the Wilson-Frenkel theory overestimate the speed of crystal growth? To address this question we propose the following scenario: We assume that the speed of crystal growth is limited by the atoms in the liquid-crystal interface region and not by the atoms in the liquid region where the liquid behaves like a bulk liquid. If this is true, one has to study the diffusion dynamics in the interface region: if diffusion in the interface region is much slower than in the bulk liquid, a failure of the Wilson-Frenkel model would be plausible since this model only

takes into account diffusive transport of the bulk liquid. To check this scenario, we have simulated inhomogeneous systems with two crystal-liquid interfaces at the melting temperature $T_m = 1520$ K. From these runs, we determined the diffusion profiles $D_{z,\alpha}(z)$ ($\alpha = \text{Ni}, \text{Al}$) along the z direction that are shown in Fig. 6 together with the number density profile. $D_{z,\alpha}(z)$ was computed from the long-time limit of the mean squared displacement in z direction,

$$D_{z,\alpha}(z_s) = \lim_{t \rightarrow \infty} \frac{1}{N_s} \sum_{i_s=1}^{N_s} \frac{\langle (z_{i_s}(t) - z_{i_s}(0))^2 \rangle}{2t}, \quad (5)$$

where z_{i_s} is the z coordinate of a tagged particle that was at time $t = 0$ in one of 30 slabs that we introduced along the z direction, each slab having a thickness of about 2.4 Å. N_s is the number of particles in slab s ($s = \{1, \dots, 30\}$). As can be seen in Fig. 6, the interface region extends over 5-6 atomic layers. Within this region the self-diffusion constants decrease roughly by about one order of magnitude. When one considers crystal growth, this slowing down of diffusion has to be taken into account, since the formation of new crystalline layers occurs in the interface region. This can be the reason why the Wilson-Frenkel model overestimates the speed of crystal growth.

Conclusions. – Extensive MD simulations have been used to investigate the crystallization kinetics as well as the diffusion dynamics of Al₅₀Ni₅₀. Although crystal growth is relatively slow in this system, the simulation yields accurate estimates of the melting temperature and the kinetic growth coefficient [for the (100) orientation of the intermetallic B2 phase]. The small value of the latter quantity, $k = 0.0025$ m/s/K, reveals that the growth kinetics of the intermetallic B2 phase is controlled by diffusive mass transport. However, the classical model for diffusion-limited growth due to Wilson and Frenkel does not give an accurate description. We argue that this is due to the neglect of diffusive transport in the crystal-liquid interface region. Microscopic theories of crystal growth shall take into account the latter diffusive processes.

* * *

Valuable discussions with Dieter Herlach and Andreas Meyer are gratefully acknowledged. We gratefully acknowledge financial support within the Priority Program 1120 Phase Transformations in Multicomponent Melts of the Deutsche Forschungsgemeinschaft (DFG). Computing time on the JUMP at the NIC Jülich and on the workstations at the ZDV (University of Mainz) is gratefully acknowledged.

REFERENCES

- [1] WILSON H.A., *Phil. Mag.*, **50** (1900) 238.
- [2] FRENKEL J., *Phys. Z. Sow.*, **1** (1932) 498.

- [3] BROUGHTON J.Q. and GILMER G.H., *J. Chem. Phys.*, **84** (1986) 5759.
- [4] BURKE E., BROUGHTON J.Q. and GILMER G.H., *J. Chem. Phys.*, **89** (1988) 1030.
- [5] BRIELS W.J. and TEPPER H.L., *Phys. Rev. Lett.*, **79** (1997) 5074.
- [6] TEPPER H.L. and BRIELS W.J., *J. Chem. Phys.*, **115** (2001) 9434.
- [7] HUITEMA H.E.A. , VLOT M.J. and VAN DER EERDEN J.P., *J. Chem. Phys.*, **111** (1999) 4714.
- [8] HUITEMA H.E.A., VAN HENGSTUM B. and VAN DER EERDEN J.P., *J. Chem. Phys.*, **111** (1999) 10248.
- [9] HOYT J.J. and ASTA M., *Phys. Rev. B*, **65** (2002) 214106.
- [10] SUN D.Y., ASTA M. and HOYT J.J., *Phys. Rev. B*, **69** (2004) 024108.
- [11] XIA Z.G., SUN D.Y., ASTA M. and HOYT J.J., *Phys. Rev. B*, **75** (2007) 012103.
- [12] JESSON B. and MADDEN P.A., *J. Chem. Phys.*, **113** (2001) 5935.
- [13] CELESTINI F. and DEBIERRE J.M., *Phys. Rev. E*, **65** (2002) 041605.
- [14] AMINI M. and LAIRD B.B., *Phys. Rev. Lett.*, **97** (2006) 216102.
- [15] TEICHLER H., *Phys. Rev. B*, **59** (1999) 8473.
- [16] ASTA M., MORGAN D., HOYT J.J., SADIGH B., ALTHOFF J.D., DE FONTAINE D. and FOILES S.M., *Phys. Rev. B*, **59** (1999) 14271.
- [17] RAMALINGAM H., ASTA M., VAN DE WALLE A. and HOYT J.J., *Int. Sc.*, **10** (2002) 149.
- [18] BECKER C.A. , OLMSTED D., ASTA M., HOYT J.J. and FOILES S.M., *Phys. Rev. Lett.*, **98** (2007) 125701.
- [19] BECKER C.A., ASTA M., HOYT J.J. and FOILES S.M., *J. Chem. Phys.*, **124** (2006) 164708.
- [20] BECKER C.A., HOYT J.J., BUTA D. and ASTA M., *Phys. Rev. E*, **75** (2007) 061610.
- [21] SIBUG-AGA R. and LAIRD B.B., *J. Chem. Phys.*, **116** (2002) 3410.
- [22] REUTZEL S., HARTMANN H., GALENKO P.K., SCHNEIDER S. and HERLACH D.M., *Appl. Phys. Lett.*, **91** (2007) 041913.
- [23] MISHIN Y., MEHL M.J. and PAPACONSTANTOPOULOS D.A., *Phys. Rev. B*, **65** (2002) 224114
- [24] DAS S.K., HORBACH J., BINDER K., KOZA M.M., MAVILA CHATHOTH S. and MEYER A., *Appl. Phys. Lett.*, **86** (2005) 011918
- [25] HORBACH J., DAS S.K., GRIESCHE A., MACHT M.-P., FROHBERG G. and MEYER A., *Phys. Rev. B*, **75** (2007) 174304
- [26] ANDERSEN H.C., *J. Chem. Phys.*, **72** (1980) 2384
- [27] ALLEN M.P. and TILDESLEY D.J., *Computer Simulations of Liquids* (Clarendon, Oxford) 1987
- [28] JACKSON K.A., *Interface Sc.*, **10** (2002) 159